Threshold Segmentation of Magnetic Column Defect Image based on Artificial Fish Swarm Algorithm

Wang Jun[1], Hou Mengjie[2]*, Zhang Ruiran[3]
Jiangxi University of Science and Technology
School of Mechanical and Electrical Engineering
Ganzhou, China

Xiao Jingjing[4]
Jiangxi Applied Technology Vocational College
School of Mechanical and Electrical Engineering
Ganzhou, China

***Abstract*—Aiming at the low efficiency of magnetic column surface defect detection, the vulnerability to human influence, and the insufficient anti-noise performance of existing 2D-OTSU threshold segmentation algorithm, an improved artificial fish swarm algorithm combined with 2D-OTSU algorithm was proposed to improve the accuracy and real-time of magnetic column surface defect detection. Firstly, the weight coefficient was added on the basis of the original 2D-OTSU algorithm, and the distance function was set to optimize the weight coefficient. The objective function was established by combining the inter-class discrete matrix and the intra-class discrete matrix, and the optimal threshold was obtained. Secondly, logistic model was used to optimize the perceptual range and moving step size of the artificial fish swarm algorithm, so as to balance the local and global search ability of the algorithm and improve the convergence speed of the algorithm. Finally, the optimal segmentation threshold is used to segment the image, and compared with other algorithms on four benchmark functions. Experimental results show that the improved algorithm can effectively reduce the time complexity of threshold segmentation and improve the efficiency of the algorithm. At the same time, the segmentation accuracy of the improved algorithm for magnetic column defects reaches 93%, which has good practicability.**

Keywords—Defect detecting; threshold segmentation; artificial fish swarm algorithm; improved 2D-OTSU algorithm

I. Introduction

In the process of magnetic column production, the surface of magnetic column will produce scarring, edge drop, black film and crack. At present, magnetic column surface defects are mainly detected and classified by inspection ,which may result in missed detection and error detection in the detection process, affecting the economic benefits of enterprises [1-2].

In recent years, image processing technology has developed vigorously, and defect detection using image processing technology has the advantages of security, reliability and strong adaptability. How to rapidly and accurately segment images by using image processing technology has become a hot topic [3]. Otsu [4] proposed the dynamic threshold method, also known as Otsu segmentation algorithm, to determine the threshold value of image segmentation by the maximum variance between the target region and background region. Zhang et al. [5] used Canny edge detection and Otsu to segment the filtered image, effectively removing the noise of abnormal points. Bo et al. [6] and Wang et al. [7]proposed to use the maximum entropy method to select segmentation threshold, when the image background is more complex, image segmentation is easy to cause partial information loss in the image and requires a large amount of calculation. The traditional Otsu algorithm only calculates the gray level of a single pixel without using the surrounding pixels, so there is a large error in the image threshold segmentation. On the basis of one-dimensional Otsu algorithm, 2D-OTSU algorithm is proposed to establish two-dimensional histogram based on the original image and the surrounding pixel smoothing information, which reduces the error in image segmentation and improves the accuracy of the algorithm.

In this paper, a threshold segmentation method of 2D-OTSU magnetic column image based on DLAFSA is proposed. By adding weight coefficient, the performance of 2D-OTSU algorithm is improved. The artificial fish swarm intelligence algorithm was introduced to improve its sensing range and moving step size, and the effectiveness of the improved artificial fish swarm intelligence algorithm was verified through performance test experiments.

II. Related Work

Liu et al. [8] proposed 2D-OTSU algorithm, which extended Otsu method to the case of two-dimensional histogram. The optimal segmentation threshold was obtained by taking the maximum straight of two-dimensional measure criterion. As the one-dimensional space changed to two-dimensional space, the amount of computation increased and the calculation speed slowed down. He et al. [9] established the one-dimensional straight-line intercept histogram and the corresponding threshold selection criterion, which improved the anti-noise performance of the algorithm, but could not distinguish the low-light position information well. Xiao et al. [10] reduced the search space of threshold by mapping the pixel set of two-dimensional histogram to the trapezoidal region, thus improving the computing efficiency. However, some information was lost when the threshold space was compressed, which reduced the segmentation accuracy. Zeng et al. [11] combined the directional fuzzy reciprocal with the straight intercept histogram, replaced the gray information of the neighborhood with the fuzzy reciprocal, strengthened the details of the weak light position, and improved the segmentation accuracy of the model. Yang et al. [12] added local variance into 2D-OTSU, which not only took into account the degree of data dispersion between each pixel point and the central pixel point, but also improved the segmentation

*Corresponding Author.

accuracy while reducing noise interference, but its operation speed was still slow.

In order to solve such problems, many studies [13-15] use swarm intelligence to improve the traditional algorithm. For example, Ma [16] proposed the swarm intelligence whale algorithm, which uses swarm intelligence to conduct local search for threshold mechanism and then further search for global extreme value, thus improving the operation speed of the algorithm. Liu et al. [17] proposed to use the improved firefly algorithm to optimize the two-dimensional Otsu algorithm. In order to enable each firefly to find its own optimal position in the global, the mobile strategy was improved and global information was introduced in the iteration to enable firefly to have global search ability, avoid falling into local extremum and improve the operation efficiency.

III. Threshold Segmentation

Threshold segmentation model has three parts, including establishing segmentation model, determining threshold criterion and solving threshold. As shown in Fig. 1(a) is the image of magnetic column surface defect to be segmented, and Fig. 1(b) is the result of segmentation of magnetic column surface image by selecting an appropriate threshold value. When the threshold value of image segmentation is an appropriate value, the target area of image defect is obvious, and the defect is completely separated from the background. When the segmentation threshold is too small, the defect region of magnetic column cannot be completely segmented, and the defect target region of magnetic column surface defect image is smaller than the actual defect area, as shown in Fig. 1(c). When the segmentation threshold is too large, the magnetic column surface defect image is over-segmented, and part of the background region of the magnetic column image is segmented into the defect region, as shown in Fig. 1(d). Therefore, determining the appropriate threshold algorithm is the key to image threshold segmentation.

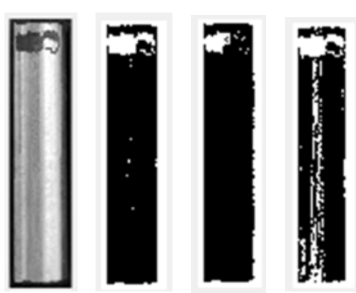

(a)Image1 (b)Image2 (c)Image3 (d)Image4.

Fig. 1. Segmentation Results of different Thresholds.

A. Improved 2D-OTSU Algorithm

In order to get the best threshold value, threshold segmentation method is very important. OTSU method is the maximum inter-class variance method, which is the criterion to determine the threshold of image segmentation [18]. However, the noise resistance of this method is weak, and the magnetic column image with low contrast is easily affected by noise, so the image segmentation effect is not obvious. In view of this, one-dimensional OTSU (1D-OTSU) method has no significant effect. Compared with 1D-OTSU, 2D-OTSU has lower sensitivity to noise and is more significant for defect image segmentation on magnetic column surface [19]. In order to eliminate the influence of isolated noise, weight coefficient is introduced, 2D-OTSU algorithm is improved to optimize the image segmentation effect.

Digital image $f(x,y)$, its field smooths the image for $g(x,y)$, $f(x,y)$ is the abscissa in a two-dimensional histogram, $g(x,y)$ is the ordinate, two-dimensional element (i,j) is composed of pixel gray value i and field gray value j, The probability is $p_{ij}=\frac{f_{ij}}{N}$. f_{ij} is the number of (i,j)'s, therefore.

$$\sum_{i=0}^{L-1}\sum_{j=0}^{L-1} f_{ij}=N,\sum_{i=0}^{L-1}\sum_{j=0}^{L-1} p_{ij}=1 \tag{1}$$

If two-dimensional element is selected as the threshold value in the two-dimensional histogram, the two-dimensional histogram can be divided into four types of regions. Region 1 and region 3 are target and background region respectively, and region 2 and region 4 are noise and edge region, respectively. The two-dimensional histogram is shown in Fig. 2.

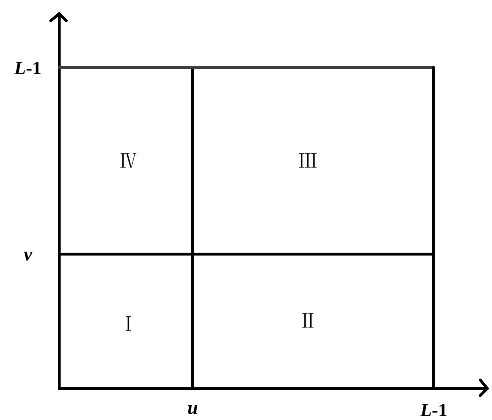

Fig. 2. Two-dimensional Histogram.

Set the probability of target and background area as ω_0 and ω_1, then

$$\omega_0=\sum_{i=0}^{u-1}\sum_{j=0}^{v-1} p_{ij},\omega_1=\sum_{i=u}^{L-1}\sum_{j=v}^{L-1} p_{ij} \tag{2}$$

The corresponding mean values η_0 and η_1 are

$$\eta_0=(\eta_{0i},\eta_{0j})^T=\left[\sum_{i=0}^{u-1}\sum_{j=0}^{v-1} ip_{ij},\sum_{i=0}^{u-1}\sum_{j=0}^{v-1} jp_{ij}\right]^T \tag{3}$$

$$\eta_1=(\eta_{1i},\eta_{1j})^T=\left[\sum_{i=u}^{L-1}\sum_{j=v}^{L-1} ip_{ij},\sum_{i=u}^{L-1}\sum_{j=v}^{L-1} jp_{ij}\right]^T \tag{4}$$

The mean value of the total gray scale is

$$\overline{\eta} = \left(\overline{\eta_i}, \overline{\eta_j}\right)^T = \left[\sum_{i=0}^{L-1}\sum_{j=0}^{L-1} i p_{ij}, \sum_{i=0}^{L-1}\sum_{j=0}^{L-1} j p_{ij}\right]^T \tag{5}$$

The various internal discrete matrices is

$$S_k = \sum_{h=0}^{L-1} \omega_k \left[\left(h-\eta_k\right)\left(h-\eta_k\right)^T\right] \quad k=0,1 \tag{6}$$

The discrete matrix between classes is

$$S = \sum_{k=0}^{1} \omega_k \left[\left(\eta_k - \overline{\eta}\right)\left(\eta_k - \overline{\eta}\right)^T\right] \tag{7}$$

The distance function between ω_0 and ω_1 is

$$r_{tr}(S) = \frac{\sum_{k=0}^{1} \omega_k \left[\left(\eta_{ki} - \overline{\eta_i}\right)\left(\eta_{kj} - \overline{\eta_j}\right)^2\right]}{\omega_0(1-\omega_0)} \tag{8}$$

When $r_{tr}(S)$ is the maximum of (i, j), two-dimensional element (u,v) is selected as the optimal threshold. However, isolated noise still exists. In order to eliminate the influence of isolated noise, this paper introduces weight coefficient β on the basis of 2D-OTSU algorithm to determine the final comprehensive objective function and obtain the optimal threshold. The objective function is determined by studying the inter-class discrete matrix and the intra-class discrete matrix:

$$r_{tr}(S) = r_{tr}(S)_{\max} - \beta r_{tr}(S_k)_{\min} \tag{9}$$

$r_{tr}(S)$ is the maximum value of $r_{tr}(S)$ between classes, $r_{tr}(S_k)_{\min}$ is the minimum value of $r_{tr}(S_k)$ within classes, and β is the weight coefficient, which is related to the grayscale characteristics of the image and can be described by ω_k. The calculation formula of weight coefficient β is as follows:

$$\beta = 1 + \frac{1-\exp(a-b\omega_k)}{1+\exp(a-b\omega_k)} \tag{10}$$

Through 200 experiments, when a=0.6, b=0.045, the best weight coefficient β is obtained, and the weight coefficient β is added into the 2D-OTSU algorithm to eliminate the influence of isolated noise.

B. 2D-OTSU Image Threshold Segmentation Method based on DLAFSA

Artificial fish swarm algorithm has strong ability to solve the optimal solution, high precision and fast convergence speed[20]. However, due to the characteristics of magnetic column defects, the traditional artificial fish swarm algorithm cannot completely meet the threshold segmentation of magnetic column surface defect image. In this paper, the artificial fish swarm algorithm is improved to improve the accuracy of threshold segmentation algorithm of magnetic column surface defect image.

1) Adjustment of perception range: The size of visual represents the size of the search area of the individual fish. When the perceptual range of visual is larger, the search range of individual fish will be larger, which is conducive to the global search. When the perceptual range is small, the local range search is more accurate.

Carry on dynamic adjustment to visual, use dynamic change form to change visual original determination way. At the beginning of the algorithm, the whole magnetic column surface image is searched globally, and the range of Visual should be enlarged to improve the convergence of the algorithm. In the later stage of the algorithm, the local search is carried out in the magnetic column surface image, and the range variation of Visual should be reduced to improve the search speed of the algorithm. The Logistic model with dynamic transformation is used to dynamically adjust Visual, set the maximum and minimum value of visual change range as $visual_{\max}$ and $visual_{\min}$, visual dynamic adjustment formula is:

$$\begin{cases} \dfrac{dvisual}{dt} = \alpha\left(1-\dfrac{visual}{visual_{\min}}\right)visual \\ visual(0) = visual_{\max} \end{cases} \tag{11}$$

According to the logistic model, formula (11) is simplified as

$$visual(t) = \frac{vidual_{\min}}{1+\left(\dfrac{visual_{\min}}{visual_{\max}}-1\right)e^{-\alpha t}} \tag{12}$$

Where, α is the initial decay rate, and t is the number of iterations of the algorithm. The initial decay rate α is used to adjust the speed of visual descent. When α is larger, it indicates that visual attenuation speed is faster, when α is smaller, it indicates that visual attenuation speed is slow.

According to (11), when the number of iterations is zero, the value of Visual is the maximum $visual_{\max}$. After t iterations, Visual approaches from the maximum value $visual_{\max}$ to the minimum value $visual_{\min}$. With the increasing number of iterations, Visual slowly converges from the maximum value $visual_{\max}$ to the minimum value $visual_{\min}$. Thus realized the algorithm from the beginning to the end of the visual value by the larger value dynamic conversion to the smaller value function.

2) Move step size adjustment: In the process of algorithm iteration, the larger step is, the faster the search speed is in the same visual. The smaller step is, the slower the search speed is and the more iterations are. At the beginning of the algorithm, visual range is larger, at this time, take a larger value of step, reduce the workload of searching the best position state, improve the convergence speed of the algorithm; In the later stage of the algorithm, the local area of the best position state has been determined, visual is a smaller search range, a smaller step is needed to carry out a more detailed local search, improve the accuracy of the algorithm.

The adjustment requirements of parameter step are the same as those of Visual, in that a larger value is required at the beginning and a smaller value is required later. The parameters change dynamically during the algorithm, from large to small. Logistic model is also used to dynamically adjust parameter step, and the formula is as follows:

$$\begin{cases} \frac{dstep}{dt} = \alpha(1-\frac{step}{step_{\min}})step \\ step(0) = step_{\max} \end{cases} \quad (13)$$

According to the Logistic model, formula (13) is simplified as:

$$step(t) = \frac{step_{\min}}{1+(\frac{step_{\min}}{step_{\max}}-1)e^{-\alpha t}} \quad (14)$$

Where, $step_{\max}$ is the maximum value of step and $step_{\min}$ is the minimum value of step.

According to the experiment, $visual_{\max}$ =10, $visual_{\min}$ =1, $step_{\max}$ =8, $step_{\min}$ =0.5, α =0.1, that is, the transformation range of Visual is [1,10], and the change range of step is [0.5,8]. The dynamic transformation curve of Visual and STEP is shown in Fig. 3.

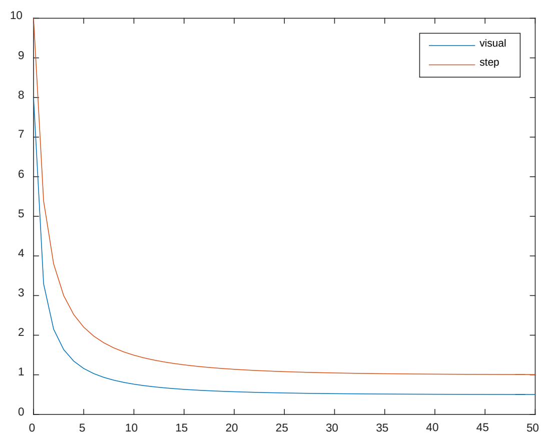

Fig. 3. Dynamic Transformation Curve of Visual and Step.

In an iterative cycle of 50, when 10 generations, visual and step convergence to the minimum, that is to say, in the first ten generations for global search, the rest of the iteration cycle for local search, this artificial fish algorithm can quickly locate the optimal solution is not at the early stage of the iteration into local optimal solution, and can improve the accuracy of solution in the late iterations.

In the 2D-OTSU algorithm, an optimal threshold (u,v) should be found for image segmentation, and the optimal threshold (u,v) should be found through the distance measure function in the maximum inter-class variance method to achieve the purpose of image segmentation of magnetic column surface defects. In this paper, 2D-OTSU algorithm is improved by adding DLAFSA algorithm to improve the accuracy and anti-noise of 2D-OTSU algorithm. The objective function of 2D-OTSU algorithm was used as DLAFSA algorithm to obtain the optimal threshold of fish food concentration $f(X)$, so as to carry out the threshold segmentation of magnetic column surface defect image.

The specific steps of 2D-OTSU image threshold segmentation based on DLAFSA are as follows:

- Initialize the algorithm parameters.
- Take the objective function of 2D-OTSU algorithm as the food concentration of DLAFSA algorithm to find the maximum distance function.
- Update the searcher position in the bulletin board to find the best position.
- Judge whether the optimal position or the condition of maximum iteration value of the algorithm is reached, and output the result; otherwise, continue to perform the previous step.
- Image threshold segmentation of magnetic column surface defects is carried out according to the optimal threshold value.

The 2D-OTSU image threshold segmentation flow chart based on DLAFSA is shown in the Fig. 4.

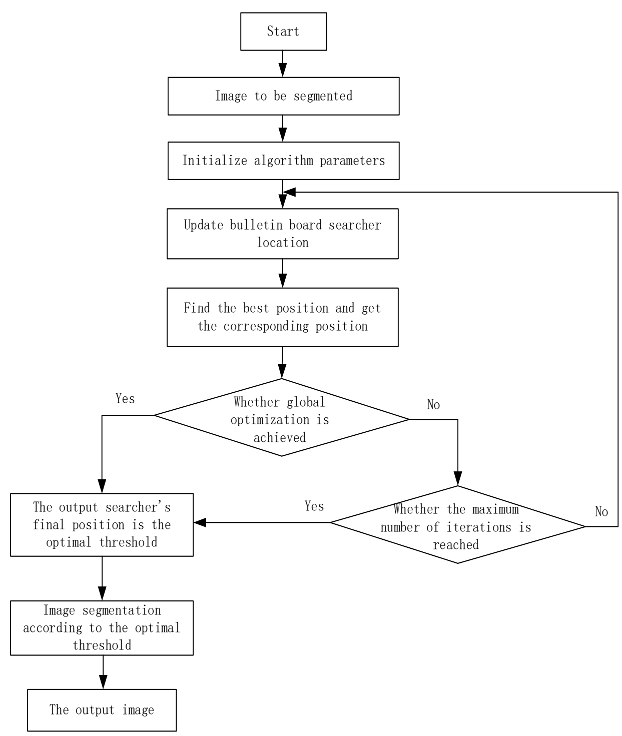

Fig. 4. 2D-OTSU Image Threshold Segmentation Flow Chart based on DLAFSA.

IV. Algorithm Performance Test

In order to verify the effectiveness of the improved artificial fish swarm algorithm, the improved adaptive artificial fish swarm algorithm DLAFSA and the standard artificial fish swarm algorithm AFSA are compared and tested by Benchmark function [19]. In DLAFSA algorithm, set parameters, n = 20, $visual_{\max}$ =10, $visual_{\min}$ =1, $step_{\max}$ =8, $step_{\min}$ =0.5, λ =2. In the AFSA algorithm, visual=2, step=2, and other parameter settings are the same as those in the DLAFSA algorithm. The four selected test benchmark functions are shown in Table I.

TABLE I. SELECTED FOUR TEST BENCHMARK FUNCTIONS

The function name	Test functions	Variable scope	The optimal value
Rastrigin	$f_1(x)=\sum_{i=1}^{n}[x_i^2-10\cos(2\pi x_i)+10]$	[-5.12,5.12]	0
Ackley	$f_2(x)=-20e^{-0.2\sqrt{\frac{1}{n}\sum_{i=1}^{n}x_i^2}}-e^{\frac{1}{n}\sum_{i=1}^{n}\cos(2\pi x_i)}+20+e$	[-50,50]	0
Rosenbrock	$f_3(x)=\sum_{i=1}^{n-1}[100(x_{i+1}-x_i^2)^2+(x_i-1)^2]$	[-32,32]	0
Schaffer	$f_4(x)=0.5+\frac{\sin^2\sqrt{x^2+y^2}-0.5}{[1+0.001(x^2+y^2)]^2}$	[-10,10]	0

The parameters of DLAFSA algorithm and AFSA algorithm are set. During the performance comparison test, both algorithms are executed for 30 times. The performance of DLAFSA algorithm is verified by comparing the mean and variance of solutions obtained by DLAFSA algorithm and AFSA algorithm after the test of four selected benchmark functions, as well as the number of successful iterations of algorithm on the benchmark function and the average number of iterations required after successful iteration.

In the four classical benchmark functions, DLAFSA and AFSA algorithms set the number of iterations to 2000. $f_1(x)$ is a unimodal function $f_2(x)$, $f_3(x)$, and $f_4(x)$ are multimodal functions. Test results of DLAFSA and AFSA on the benchmark function are shown in Table II.

As can be seen from the data results in Table II, the mean values of solutions obtained from four different benchmark functions are smaller than those obtained from AFSA algorithm. Compared with AFSA algorithm, the variance of solutions obtained by DLAFSA algorithm in four different benchmark functions is smaller. From the comparison of mean and variance, DLAFSA algorithm has higher accuracy, and DLAFSA algorithm is better than AFSA algorithm.

TABLE II. TEST RESULTS OF DLAFSA AND AFSA ON THE BENCHMARK FUNCTION

Benchmark functions	DLAFSA		AFSA	
	The mean	The variance	The mean	The variance
f_1	1.4203	0.2912	12.6237	2.7212
f_2	5.6e-16	8.1e-16	2.8e-10	1.9e-12
f_3	1.7e-28	2.7e-72	0.00681	0.0143
f_4	3.5231	2.7873	6.6372	3.8221

TABLE III. SUCCESSFUL ITERATION RESULTS OF DLAFSA AND AFSA

Benchmark functions	DLAFSA		AFSA	
	Number of successful	Average number of iterations	Number of successful	Average number of iterations
f_1	21	1074	15	1829
f_2	16	1527	9	1672
f_3	23	982	23	1082
f_4	28	609	19	695

Table III shows the average iteration times required by DLAFSA algorithm and AFSA algorithm for successful iteration on benchmark functions when the test results and algorithm convergence are successful. It can be seen from the table that the successful iteration times of DLAFSA algorithm on four benchmark functions are more than the successful iteration times of AFSA algorithm on four benchmark functions. The average iteration times of DLAFSA algorithm on the successful iteration of the four benchmark functions are also less than that of AFSA algorithm on the successful iteration of the four benchmark functions. The performance of DLAFSA algorithm is better than that of AFSA algorithm.

V. EXPERIMENTAL RESULTS AND ANALYSIS

In order to verify the effect and accuracy of the improved 2D-OTSU image threshold segmentation method on magnetic column surface defect image threshold segmentation, the 2D-OTSU image threshold segmentation method based on DLAFSA was compared with the traditional 2D-OTSU method and the improved firefly algorithm in literature [21]. The image segmentation of four magnetic column surface defects, namely, magnetic column scar, black slice, edge drop and crack, was analyzed by comparative experiment. The image threshold segmentation and comparison effect of magnetic column surface defects is shown in Fig. 5.

As can be seen from the comparison figure, magnetic column surface defects are complex and have many kinds of defects. For scarring and black spot defects, the traditional 2D-OTSU algorithm will produce many noise points. Although the algorithm in [21] effectively reduces noise points, the edge segmentation effect of magnetic column is poor. For side drop defects, the 2D-OTSU algorithm has more noise points, and both the algorithm in [21] and the algorithm in this paper can be well segmented. However, for crack defects with low contrast, the traditional 2D-OTSU image segmentation algorithm and the algorithm in [21] are still affected by isolated noise and cannot effectively extract magnetic column surface defects. However, the algorithm in this paper can effectively eliminate isolated noise and extract magnetic column surface defects. Table IV shows the comparison of optimal thresholds and time for processing magnetic columns with different defects using three threshold segmentation algorithms. It can be seen that the running time of 2D-OTSU using firefly algorithm is 32.2% of that of traditional 2D-OTSU. Although it can effectively reduce the running time, the running speed is still relatively slow. The proposed algorithm reduces the running time of the traditional 2D-OTSU algorithm by 82.45%, and ensures the accuracy of the algorithm while reducing the running time.

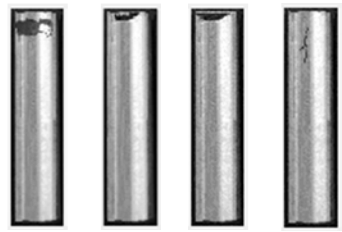

(a) Scar (b) Black piece (c) Off the edge (d) Cracks
（1）Image to be segmented

(a) Scar (b) Black piece (c) Off the edge (d) Cracks
(2) Traditional 2D-OTSUalgorithm

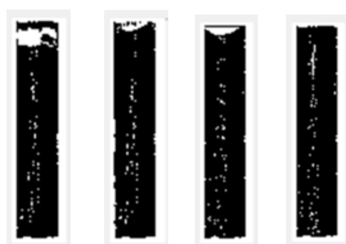

(a) Scar (b) Black piece (c) Off the edge (d) Cracks
(3) Literature [21] improved firefly algorithm

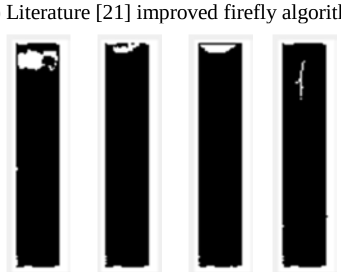

(a) Scar (b) Black piece (c) Off the edge (d) Cracks
(4) Algorithm in this paper

Fig. 5. Threshold Segmentation Effect of different Methods.

TABLE IV. THE OPTIMAL THRESHOLD AND SEGMENTATION TIME OF DIFFERENT ALGORITHMS ARE COMPARED

Algorithm	Scar	Black piece	Off the edge	Cracks	Mean Spent time/ms
2D-OTSU	(96,109)	(102,123)	(94,115)	(103,117)	508.43
Firefly algorithm + 2D-OTSU	(103,112)	(109,120)	(106,112)	(102,115)	163.59
Ours	(103,108)	(113,119)	(108,112)	(107,111)	89.23

The threshold segmentation of 500 magnetic column images with defects is carried out by the method in this paper, and the images obtained are used as classification recognition samples after feature extraction. 300 of them are selected as KNN classifier training sample set, and the remaining 200 as KNN classifier test sample set. The test samples are classified by the KNN classifier successfully trained. The classification recognition results are statistically analyzed, and the classification results are shown in Table IV.

TABLE V. CLASSIFICATION RESULTS

	Scar	Black piece	Off the edge	Cracks	total
Actual sample size	45	55	48	52	200
Correct identification number	41	52	44	49	186
Leaving out the number	0	0	0	0	0
Mistakenly identified several	2	2	1	1	6
Recognition accuracy%	91.1	94.5	91.7	94.2	93

Table V shows that the classification accuracy of four types of magnetic column surface defects reaches 93%, including 94.5% for black piece defects, the accuracy of cracks defect classification was 94.2%. Due to the difficulty in distinguishing edge defect from scar defect, the classification accuracy is lower than the other two defect types, but the recognition accuracy can reach more than 90%. The recognition accuracy of scar is 91.1%, the recognition accuracy of off the edge is 91.7%. In particular, the missing rate is 0, and all defects can be detected, which can meet the requirements of magnetic column surface defect detection.

VI. CONCLUSION

Aiming at the problems of low segmentation efficiency and weak anti-noise ability of traditional 2D-OTSU algorithm, this paper proposes a 2D-OTSU image threshold segmentation algorithm based on DLAFSA. In this paper, a weight coefficient is added to 2D-OTSU algorithm to eliminate isolated noise and distinguish background and target effectively. The artificial fish swarm algorithm is improved to improve the convergence and search speed of the algorithm and effectively reduce the time complexity of threshold segmentation by adjusting the perceived range and moving step size of fish swarm. By comparing the performance of adaptive artificial fish swarm algorithm DLAFSA with the standard artificial fish swarm algorithm AFSA using the benchmark function, it is concluded that the improved algorithm has higher accuracy, shorter convergence time and stronger overall performance than the original algorithm. Finally, the proposed algorithm is compared with the traditional 2D-OTSU method and the improved firefly algorithm in terms of segmentation accuracy and running time. Experimental results show that the proposed algorithm can better segment magnetic column edge, effectively eliminate isolated noise, improve the running speed of the algorithm, and ensure the segmentation accuracy.

AKNOWLEDGMENT

This work is supported by science foundation of Education Department of Jiangxi Province(GJJ150676), and Natural science foundation of Jxust(NSFJ2015-G15).

References

[1] Song Ke, Xie Weicheng, Xia Xingyang,and Jiang Wenbo. Research on Wallpaper Defect Detection Method Based on improved Otsu [J]. Manufacturing Automation,2019, Vol. 41 (6): 12-15.

[2] Da Yihui, Dong Guirong, Wang Bin, Liu Dianzi, and Qian Zhenghua. A novel approach to surface defect detection[J]. International Journal of Engineering Science, 2018, 133(DEC.):181-195.

[3] Zhao Feng, Kong Lingrun, and Ma Geni. Threshold image segmentation algorithm based on hybrid optimization of multi-objective particle swarm optimization and artificial bee swarm optimization [J]. Computer engineering and science,2020,42(02):281-290.

[4] Aditya Raj, Gunjan Gautam, Siti Norul Huda Sheikh Abdullah, Abbas Salimi Zaini, and Susanta Mukhopadhyay. Multi-level thresholding based on differential evolution and Tsallis Fuzzy entropy[J]. Image and Vision Computing,2019,91: 103792.

[5] Zhang Zhenhai, Jia Zhengman, Ji Kun. Research on Crack Identification Method of Subway tunnel based on improved Otsu Method [J]. Journal of Chongqing Jiaotong University (Natural Science Edition),2022, Vol. 41 (1): 84-90.

[6] Lei Bo, Fan Jiulun. Image thresholding segmentation method based on minimum square rough entropy[J]. Applied Soft Computing, 2019, 84(1):105687.

[7] Wang Yun, Zhang Guangbin, and Zhang Xiaofeng. Multilevel Image Thresholding Using Tsallis Entropy and Cooperative Pigeon-inspired Optimization Bionic Algorithm[J]. Journal of Bionic Engineering, 2019, 16(5): 954-964.

[8] Liu Jianzhuang, Li Wenqing. Two-dimensional Otsu Automatic Threshold Segmentation method for Gray Image [J]. Acta Automatica Sinica,1993(01):101-105.

[9] He Zhiyong, Sun Lining, Huang Weiguo. Thresholding segmentation method based on Otsu Criterion and line Intercept histogram[J]. Optics and Precision Engineering, 2012, 20(10):2315-2323.

[10] Xiao Leyi, Ouyang Honglin, Fan Chaodong. An improved Otsu method for threshold segmentation based on set mapping and trapezoid region intercept histogram[J]. Optik, 2019, 196:163106.

[11] Zeng Yanyang, Xie Gaosen, and Zhang Jianchun. Low-light image segmentation based on intercept histogram and Otsu fusion [J]. Laser & Optoelectronics Progress,2021, vol 58 (20): 219-227.

[12] Yang Huixian, Yan Wei, Tan Zhenghua, Li Miao, and Cai Yongyong. Image segmentation based on improved gray local variance[J].Computer Engineering and Applications.2017,53(4):209-213.

[13] Cao Shuang, An Jiancheng. Wolf Optimized 2D Otsu Fast Image Segmentation Algorithm [J]. Computer Engineering and Science, 2018, Vol. 40 (7):1221-1226.

[14] Zhang Lin, Wang Tinghua, and Zhou Huiying. Research Progress of SVR Parameter Optimization Based on Swarm Intelligence Algorithm [J]. Computer Engineering and Applications, 2021, Vol 57 (16):50-64.

[15] Yan Yuanyuan, Chen Hua, and Jiang Bo. Identification of tomato diseases based on swarm intelligence algorithm classification model [J]. Jiangsu Agricultural Sciences,2020, Vol 48 (1): 219-224.

[16] Ma Guoyuan, Yue Xiaofeng. An improved whale optimization algorithm based on multilevel threshold image segmentation using the Otsu method[J].Engineering Applications of Artificial Intelligence,2022,Vol.113: 104960.

[17] Liu Peijin, Wang Xi, and He Ning. Improved multi-threshold infrared image segmentation method based on FUSION of GSO and TWO-DIMENSIONAL OTSU [J]. Journal of Applied Optics, 2021, Vol.42 (4):671-677.

[18] Numan Saeed , Nelson King , Zafar Said , and Mohammed A. Omar. Automatic defects detection in CFRP thermograms, using convolutional neural networks and transfer learning[J]. Infrared Physics & Technology, 2019, 102:103048.

[19] Cao Yiqin, Duan Yeyu, and Wu Dan. Image segmentation method of 2d-otsu rail defects based on WFSOA [J]. Computer science,2020,47(5):154-160.

[20] Cui Liqun, Song Xiao, Li Hongxu, Zhang Mingjie. Multi-threshold image segmentation based on improved fish swarm algorithm [J]. Computer science,2014,41(08):306-310+321.

[21] Liu Xinjing, Liu Yanlong, and Xu Xinxin. Membrane mechanism Firefly algorithm optimization of Multi-threshold Otsu image Segmentation [J]. Journal of Small And Micro Computer Systems,2020, Vol 41 (2): 410-415.